Free Radical Research, December 2009; 43(12): 1225–1239

informa
healthcare

RESEARCH PAPER

Protective signalling effect of manganese superoxide dismutase in hypoxia-reoxygenation of hepatocytes

MICHAL PARDO & OREN TIROSH

Institute of Biochemistry, Food Science and Nutrition, Robert H. Smith Faculty of Agriculture, Food and Environment, The Hebrew University of Jerusalem, Rehovot 76100, Israel

(Received 21 June 2009; In revised form date 19 August 2009)

Abstract
This study investigates the mechanism by which MnSOD exerts its protective effect in hypoxia-reoxygenation (H/R) injury in hepatocytes. Following induction of H/R, MnSOD expression and activity levels increased and remained high for over 24 h. Hepatocytes silenced for MnSOD (siMnSOD) demonstrated increased susceptibility to H/R-induced apoptotic cell death and a lower capacity to generate mitochondrial reactive oxygen species. Microarray and real time PCR analysis of gene expression from siMnSOD cells revealed a number of down-regulated protective genes, including hemeoxygenase-1, glutamate-cysteine ligase and Nrf2, a master regulator of cellular adaptation to stress. Decreased Nrf2 protein expression and nuclear translocation were also confirmed in siMnSOD cells. siMnSOD cells showed low glutathione (GSH) content with no oxidation to GSSG, lower lipid peroxidation levels than their controls and lower mitochondrial membrane potential, which all were even more salient after H/R. Therefore, MnSOD appears to act as a signalling mediator for the activation of survival genes following H/R injury in hepatocytes.

Keywords: *Apoptosis, microarray, reactive oxygen species, redox signaling, mitochondrial defense*

Introduction

Hypoxia-reoxygenation (H/R) is an important mechanism of cellular injury in transplantation and in myocardial, hepatic, intestinal, cerebral, renal and other ischemic syndromes. Cellular hypoxia and reoxygenation are two essential elements of ischemia-reperfusion (I/R) injury. Oxidative stress arising from excessive production of reactive oxygen species (ROS) has long been associated with I/R injury [1,2].

Manganese superoxide dismutase (MnSOD, SOD2) is an essential primary antioxidant enzyme that converts superoxide radicals and protons to hydrogen peroxide (H_2O_2) within the mitochondrial matrix, generated by respiratory chain activity [3]. Several reports have demonstrated a protective role for MnSOD in I/R [4,5]. However, the signalling mechanisms by which MnSOD exerts its protective effect in H/R are still unknown.

Accumulating evidence indicates that the mitochondria play a pivotal role in cell death in response to I/R. Mitochondria isolated from I/R livers have impaired function [2,6]: decreased adenine nucleotides content, depressed activity of respiratory chain complex, lower mitochondrial membrane potential ($\Delta\psi m$) and decreased nicotinamide adenine dinucleotide (NADH) dehydrogenase activity. Mitochondrial dysfunction results in mitochondrial Ca^{2+} overload, free radical production, decreased respiratory activity and, ultimately, induction of cell death [2,6]. Accordingly, mitochondria may contribute to many

Correspondence: Michal Pardo, The Hebrew University, Faculty of Agriculture, Department of Biochemistry and Nutrition, PO Box 12, Rehovot, Israel. Fax: +972 8 9363208. Email: pardo@agri.huji.ac.il

ISSN 1071-5762 print/ISSN 1029-2470 online
DOI: 10.3109/10715760903271256

signal-transduction pathways via regulation of Ca^{2+} and ROS production, both tightly connected to the $\Delta\psi m$ [7].

Mitochondria from heterozygous mice with a partial knockout of MnSOD have shown evidence of increased proton leakage, inhibition of respiration, declines in mitochondrial function and early and rapid accumulation of mitochondrial oxidative damage [8]. Therefore, the objective of the present study was to investigate whether MnSOD, a member of the antioxidant defence system, regulates ROS production in response to H/R and thereby modulates different key signalling pathways in hepatocytes.

Another important mechanism by which cells adapt to oxidative stress involves upregulation of a distinct array of cytoprotective genes responsible for the cells' antioxidant capacity [9,10]. Some of these genes act to maintain glutathione (GSH) content and activity; they are also responsible for detoxification of damaging electrophilic by-products of oxidant stress and include glutathione S-transferases, aldehyde dehygrogenases and NAD(P)H quinone oxidoreduc-tases (NQO1) [11]. A master regulator of this specific antioxidant phenotype is the transcription factor NF-E2-related factor-2 (Nrf2) [11,12]. Under conditions of oxidative stress, Nrf2 is activated, then accumulates and localizes to the nucleus, where it heterodimerizes with specific cofactors, including members of the Maf protein family, and coordinates upregulation of cytoprotective genes through the transactivation of antioxidant response elements (AREs) within the regulatory regions of these genes [12]. Several studies have determined a role for Nrf2 in mediating responses to H/R [9,13].

In this study, a stable silencing system for the MnSOD gene in hepatocytes was used to study the role of MnSOD in H/R. We observed down-regulation of Nrf2-dependent gene expression in MnSOD-silenced cells. These are the first data to demonstrate that MnSOD-mediated protection against H/R may be coordinated by Nrf2.

Materials and methods

Preparation of MnSOD-silenced cells

Wild type (WT)-AML-12 (ATCC No. CRL-2254™) cells silenced (si) for MnSOD were prepared as previously described [4]. pSUPER.retro.puro was used with transcripts of 60-nt long designed to generate a low level of MnSOD silencing. Retroviral particles were produced by triple transfection of HEK 293T cells (ATCC No. CRL-11268™) with the retroviral vector (2 μg), pMD-gag-pol (1 μg) and pVSV-G (1 μg) using Trans-IT (Mirusbio Corporation, Madison, WI). For stable transfection selection was made with 10 μg puromycin for 2 weeks.

Cell culture and H/R conditions

WT-AML-12 mouse hepatocytes and cells stably silenced for MnSOD (siMnSOD) and their no-sense-Scramble-control (Scr-control) were grown in Dulbecco's modified Eagle's medium (DMEM) supplemented with 10% (w/v) fetal calf serum, 50 μg/ml gentamycin, 100 mg/ml kanamycin and 1% (w/v) glutamine at 37°C in a humidified atmosphere consisting of 95% air and 5% CO_2. Hypoxic conditions of 1% O_2 were attained as was previously described [4,14], using a commercially available hypoxia chamber (MIC-101, Billups-Rothenberg, Del Mar, CA) for 6 or 24 h.

Gene expression: RNA isolation, cDNA synthesis and real-time PCR

Total RNA was extracted from WT-AML-12, Scr-control and siMnSOD hepatocytes using TRI reagent (Sigma-Aldrich). One microgram of extracted RNA was reverse-transcribed (RT) using an RT kit (Applied Biosystems, Foster City, CA), real-time PCR was performed using the SYBR Green PCR mix in an ABI Prism 7300 Sequence Detector System (Applied Biosystems). β mRNA was used as an endogenous control. Primers were purchased from Hy-Laboratories Ltd. (Rehovot, Israel) (Table I).

Gene chip probe array analyses

To identify sets of genes that are differentially expressed in siMnSOD AML-12 cells compared to Scr-control AML-12 cells, a gene chip approach was utilized. Total RNA was extracted (using TRI reagent) and purified using the RNeasy kit (Qiagen, Valencia, CA).

Table I. Primers used for qPCR analysis of gene expression.

Gene	Primer
MnSOD (mouse)	Left: 5′-CAC ACC ATT TTC AGG ACA AAC-3′
(NM_013671)	Right: 5′-TTC TCA AAA GAC CCA AAG TCA-3′
HO-1 (mouse)	Left: 5′-CTC TCT GGA ATG GAG GGA GA-3′
(NM_010442)	Right: 5′-GCT GCT GGT TTC AAA GTT CA-3′
GCLC (mouse)	Left: 5′-CGA GGT GGA GTA CAT GTT GG-3′
(NM_010295)	Right: 5′-TCG CCT CCA TTC AGT AAC AA-3′
Nrf-2 (mouse)	Left: 5′-GCA TGA TGG ACT TGG AGT TG-3′
(NM_010902)	Right: 5′-GTC TTG CCT CCA AAG GAT GT-3′
β-Action (mouse)	Left: 5′-CTA AGG CCA ACC GTG AAA AG-3′
(NM_007393)	Right: 5′-GGG GTG TTG AAG GTC TCA AA-3′

Microarray analysis was performed on an Affy-metrix Mouse Gene 1.0 ST chip containing 28 853 genes. The chips were processed and scaled at the Weizmann Institute of Science (Rehovot, Israel) using Affymetrix MAS5. Statistical analysis of microarray data was performed using the Partek® Genomics Suite (Partek Inc., St. Louis, MI) software. CEL files (containing raw expression measurements) were imported to Partek GS. The data were pre-processed and normalized using the robust multichip average (RMA) algorithm [15]. The normalized data were explored by principal components analysis (PCA) and hierarchical clustering. To identify differentially expressed genes, one-way ANOVA was applied. False discovery rate (FDR) was used to correct for multiple comparisons [16]. Functional annotation was determined using the NCBI program DAVID and the Web-based GEne SeT AnaLysis Toolkit (WEBGESTALT) of Vanderbilt University. (Gene chip presented in public domain, Expression Omnibus accession no. GSE14855.)

Western-blot analysis, Coomassie staining and protein identification by mass spectrometry (MS)

Total proteins from cells were extracted using two times boiling in lysis buffer (1% sodium dodecyl sulphate (SDS), 1 mM sodium orthovanadate, 10 mM Tris, pH 7.4). Proteins were analysed by SDS-PAGE using a Bio-Rad (Hercules, CA) electrophoresis system. Immunoblotting was performed according to manufacturer's instructions. Mouse anti-MnSOD and mouse anti-β antibodies were purchased from BD Biosciences (Franklin Lakes, NJ), rabbit anti-Nrf2 was purchased from Santa Cruz Biotechnology (Santa Cruz, CA) and mouse anti-4-hydroxynonenal (4-HNE) antibody was purchased from R&D Systems Inc. (Minneapolis, MN). Immu-noreactive bands were visualized with enhanced che-miluminescence light-detection reagents (Santa Cruz Biotechnology). Several other gels were stained with Coomassie Brilliant Blue and a band at 65–70 kDa was excised and sent to the Smoler Proteomic Center, Department of Biology, Technion (Haifa, Israel) for protein identification by MS and was identified as albumin.

In-gel activity assay

In-gel activity assay for MnSOD activity was performed as previously described [17].

Nrf2 localization

Scr and siMnSOD cells were grown in eight chamber cover-slips. Cells were fixed in 100% methanol at –20°C for 10 min. Fixed cells were incubated with anti-Nrf2 antibody (Santa Cruz Biotechnology) at 4°C overnight. Subsequently, cells were incubated with FITC-labelled secondary antibody (Jackson ImmunoResearch Laboratories, West Grove, PA) (dilution 1:250) at room temperature for 1 h. Nuclear integrity was determined by incubation with 10 ng 4′-6-diamidino-2-phenylindole (DAPI) solution for 15 min. Sections were examined by a Leica CLSM (DMI4000 B Inverted Microscope, Meyer Instruments, Houston, TX). For western blot analysis of Nrf2 in different cellular compartments, fractionation of nuclear and cytosolic extracts were performed as previously described [4].

Determination of cell viability

The DNA interchelating dye propidium iodide (PI), which is excluded by viable cells, was used. Flow cytometer (FACSCalibur, BD, Foster City, CA) analysis was used to evaluate cell viability, at the following fluorescence settings: excitation at 488 nm and emission at 575 nm. Data were collected from 10 000 cells.

Caspase 3-like (DEVDase) activity

Analysis of caspase 3-like activity was carried out as was previously described [17] using 60 μM fluorogenic caspase-3 substrate (Ac-DEVD-AMC, Calbiochem, La Jolla, CA). Fluorescence was recorded using a microfluorometer plate reader (GENios, Tecan, Salzburg) at 360 nm excitation and 460 nm emission.

DNA integrity

Following exposure to H/R, cells fixated in 1% (w/v) paraformaldehyde, centrifuged (500 g, 5 min) and resuspended in a solution containing 50 μg PI/ml, 0.1% (w/v) sodium citrate and 0.1% Triton X-100. The permeabilized cells were kept in the dark at 4°C for 1 h and analysed by flow cytometry; excitation 488 nm, emission at 575 nm. Data were collected from 10 000 cells.

Measurement of intracellular ROS

H_2O_2 were detected using a dichlorodihydrofluorescein diacetate (H_2DCF-DA) fluorescent probe as previously described [17].

Determination of mitochondrial membrane potential, $\Delta\psi m$

$\Delta\psi$m was determined using JC-1 dye and a dual-emission potential-sensitive probe. In cells with high $\Delta\psi$m, JC-1 spontaneously forms complexes known as

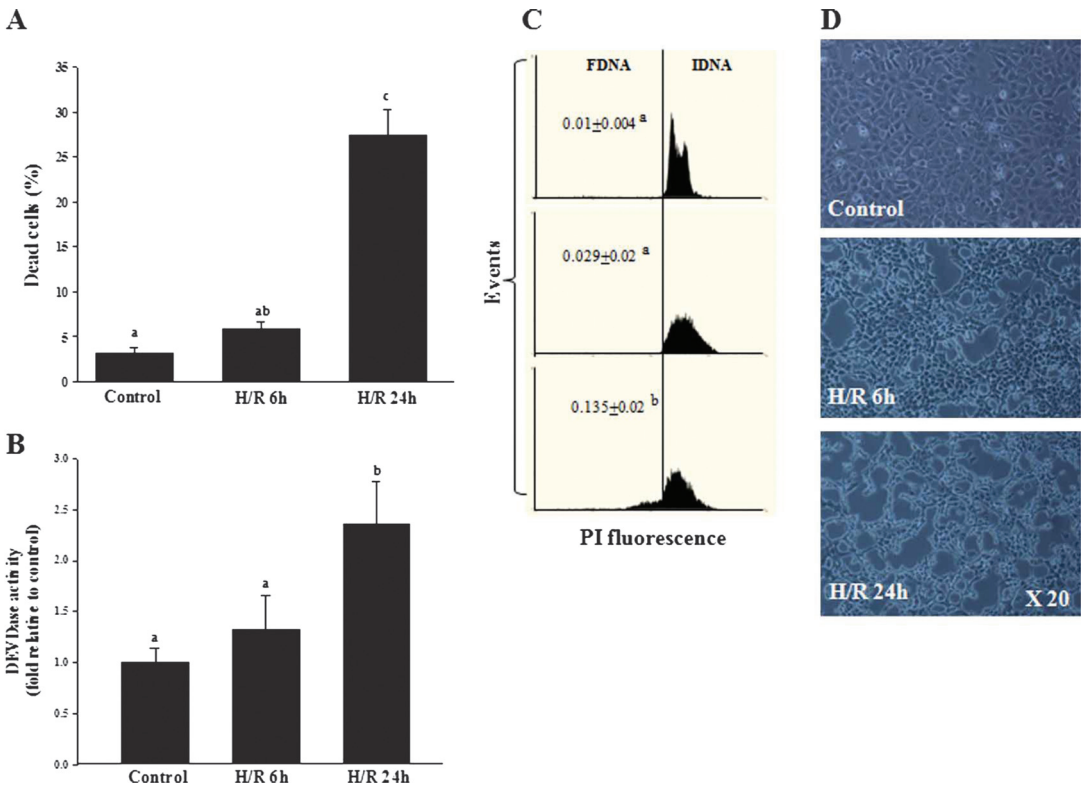

Figure 1. H/R of AML-12 hepatocytes induces apoptotic cell death. Cells were exposed to H/R. (A) Fraction of dead PI-positive cells detected by flow cytometry (FACSCalibur, BD). (B) DEVDase (caspase) activity measured by fluorogenic specific caspase-3 substrate. (C) DNA integrity detected by flow cytometry, using permeable cells and PI staining. Numbers represent the ratio between fragmented DNA (FDNA) and intact DNA (IDNA). Means with different letters are significantly different at $p < 0.05$, $n = 5$. Histograms are representative of two separate experiments, $n = 5$ per experiment. (D) Cells were photographed under a light microscope. Images are representative of cells from four different experiments.

J-aggregates with intense red fluorescence at 560 and 595 nm. To stain cells for $\Delta\psi m$, the JC-1 Mitochondrial Membrane Potential Assay Kit was purchased from Cayman Chemical Company (Ann Arbor, MI) and used according to the manufacturer's instructions for flow cytometry analysis. For WT-AML-12 cells treated with carbonyl cyanide 3-chlorophenylhydrazone (CCCP) (Sigma-Aldrich), CCCP was added 5 min after staining with JC-1. Data were collected from 10000 cells. The change in $\Delta\psi m$ was measured by the loss of red fluorescence.

Preparation of sample standards and GSH measurement by high-performance liquid chromatography (HPLC)

All cells and standards (GSH and GSSG, Sigma-Aldrich) were prepared as was previously described [18]. GSH and GSSG concentrations were measured by HPLC with online electrochemical detection. Stationary phase: Reverse-phase Phenomenex Synergi column (250 mm × 4.6 mm × 4 µm) (Torrance, CA). Mobile phase: 2% (v/v) acetonitrile in 50 mM KH_2PO4 pH 2.7. GSH and GSSG were detected with an ESA Coulochem II electrochemical coulometric detector (Bedford, MA) with a 5011 analytical cell run in oxidative mode (+ 850 mV). The flow rate for elution was maintained at 0.5 ml/min by an ESA pump.

Statistical analysis

Results are expressed as mean ± standard deviation of the mean (SD). The difference between two group means was tested by Student's *t*-test and one-way ANOVA was used in multivariable analyses. Differences were considered significant at a probability level of $p < 0.05$ using the Fisher's protected least-significant difference method.

Results

H/R-induced apoptosis in AML-12 hepatocytes

H/R is a pathological stress that may activate cell-death pathways. To determine the extent of hepatocyte damage following 6 and 24 h of H/R, cells were stained with PI: ~8 and 30% of the cells stained PI-positive, respectively, and were considered dead (Figure 1A). To determine the type of cell death prevailing in H/R, caspase activity and DNA-fragmentation levels were assessed. Following 6 and 24 h of H/R, caspase activity was increased relative to control

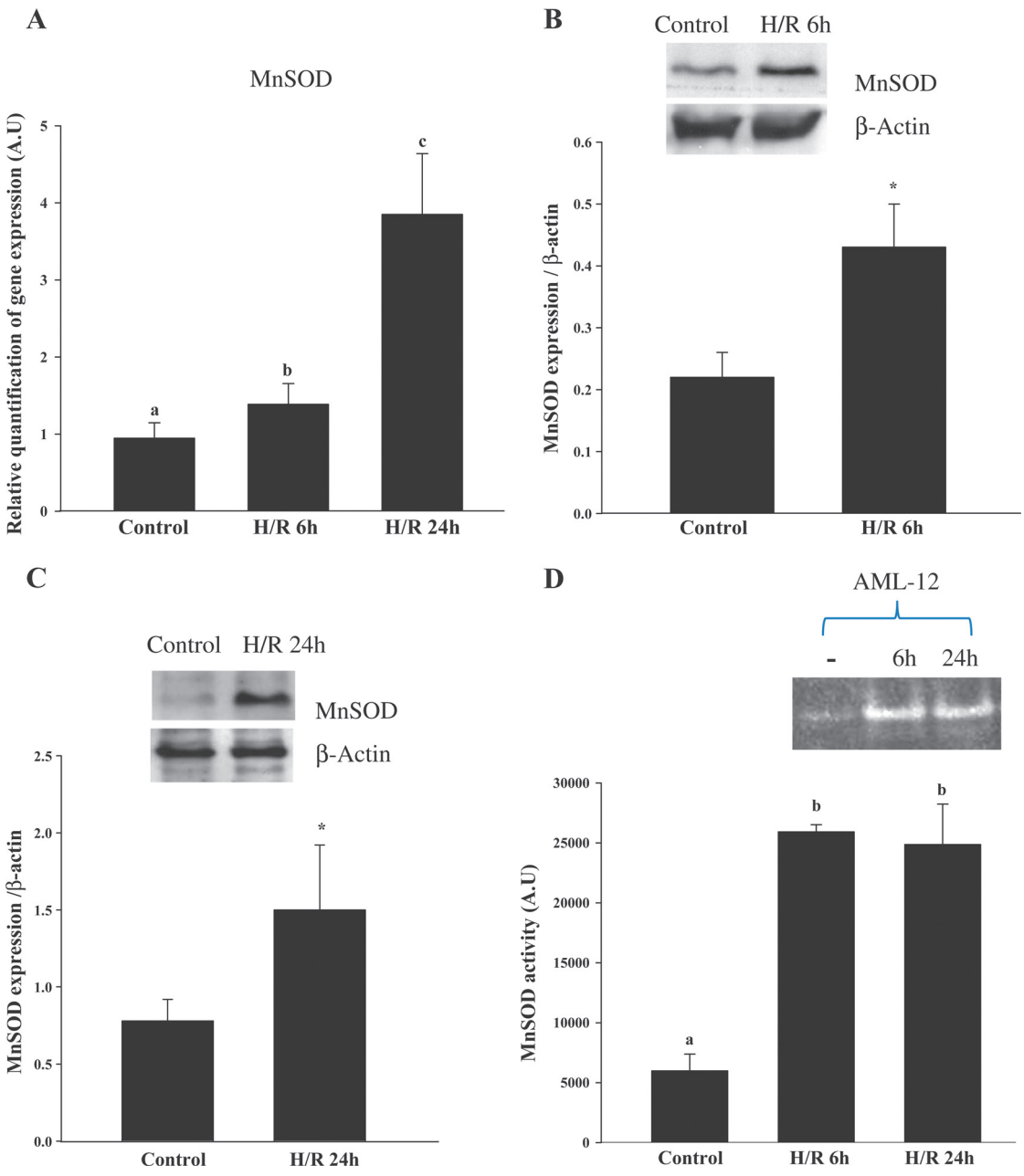

Figure 2. MnSOD expression is increased after H/R. Cells were exposed to H/R. (A) Quantitative analysis was performed by RT and realtime PCR for mRNA levels of MnSOD. Values are expressed as fold change of gene expression compared to a calibrator (endogenous control, *β*). Means with different letters are significantly different at $p < 0.05$. MnSOD expression was analysed by immunoblotting with antibodies against MnSOD and calibrating to *β*. (B) Analysis after 6 h of H/R and (C) 24 h of H/R. Data represent means ± SD; *significantly higher at $p < 0.05$ than controls. (D) Enzymatic activity of MnSOD was tested on cyanide-treated in-gel assay from cell. Means with different letters are significantly different at $p < 0.05$. These experiments were performed in triplicate and were repeated twice.

cells, suggesting damage due to apoptotic cell death (Figure 1B). The level of fragmented DNA, another characteristic feature of apoptosis, was also higher following H/R (Figure 1C). Furthermore, images taken following H/R showed the cells' tendency to shrink and cluster together, creating apparent voids in their monolayer structure. This observation was not recorded in control cells (no H/ R) or in cells prior to H/R (Figure 1D). Thus, H/R leads to damage and cell death and the type of cell death is of apoptotic characteristics.

MnSOD expression is increased after H/R

Mitochondrial MnSOD levels in rat liver are upregulated as a protective adaptive mechanism following I/R [4]. In hepatocytes exposed to 6 or 24 h of H/R realtime PCR revealed a 50 and 400% increase in MnSOD mRNA levels, respectively (Figure 2A). MnSOD protein levels were evaluated by western-blot analysis of cell lysates following exposure to H/R. In correlation with the increase in mRNA levels, MnSOD protein levels were upregulated by 100%

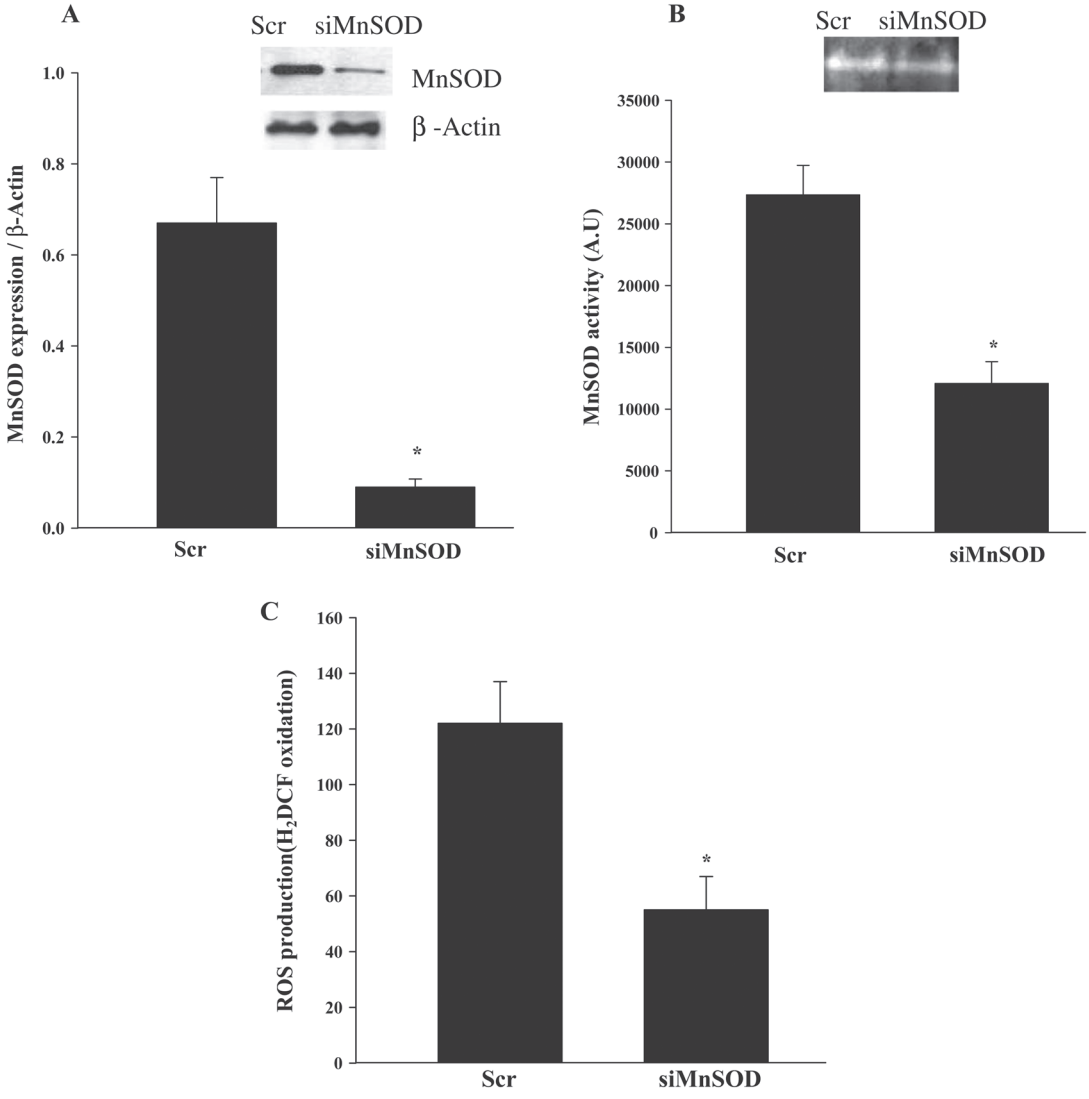

Figure 3. AML-12 hepatocytes silenced for MnSOD expression. WT-AML-12 cells were silenced using the retrovirus system, generating silenced cells for MnSOD expression (siMnSOD) and a scrambled-no gene recognition control sense (Scr-control). (A) MnSOD expression levels were analysed by immunoblotting with antibodies against MnSOD and β. (B) Enzymatic activity of MnSOD was tested on cyanide-treated in-gel assay with cell lysates. (C) Intracellular ROS were measured using H2DCF-DA by flow cytometry. Data represent means ± SD; *significantly lower at $p < 0.05$ than controls. These experiments were performed in triplicate and were repeated twice.

after 6 h of H/R compared to control cells (Figure 2B). Moreover, an increase of similar magnitude in MnSOD levels was also evident after 24 h of H/R (Figure 2C). MnSOD activity was analysed in H/R and control cell lysates. H/R caused a 500% increase in mitochondrial MnSOD levels of activity after 6 and 24 h of H/R (Figure 2D). All together, MnSOD transcription, expression and activity at both 6 and 24 h after H/R were higher than control. The prolonged elevated protein levels and activity of MnSOD suggest a protective role for this protein in hepatocyte recovery following H/R.

siMnSOD AML-12 hepatocytes generate less H_2O_2 and are more sensitive to H/R-induced cell death

To determine whether the upregulation of MnSOD levels plays a physiological role in protecting against H/R injury, WT-AML-12 hepatocytes were silenced for MnSOD using a retrovirus system. shRNA construct specifically targeting MnSOD transcript selectively silenced MnSOD (siMnSOD) protein expression (by 95%); shRNA scramble construct (Scr) was used as a control for non-silenced RNA interference (Figure 3A). MnSOD activity analysis by cyanide-treated in-gel assay of lysates from siMnSOD and Scr-control cells revealed a significant decrease in mitochondrial MnSOD activity (Figure 3B). Cellular ROS production was evaluated using H_2DCF-DA oxidation in siMnSOD cells and their Scr-controls: siMnSOD cells exhibited lower H_2O_2 production capacity (Figure 3C). In response to H/R, siMnSOD cells died more readily*45% PI-positive siMnSOD cells compared to 22% Scr-control cells (Figure 4A). Caspase activity increased after H/R as well (at 6 and

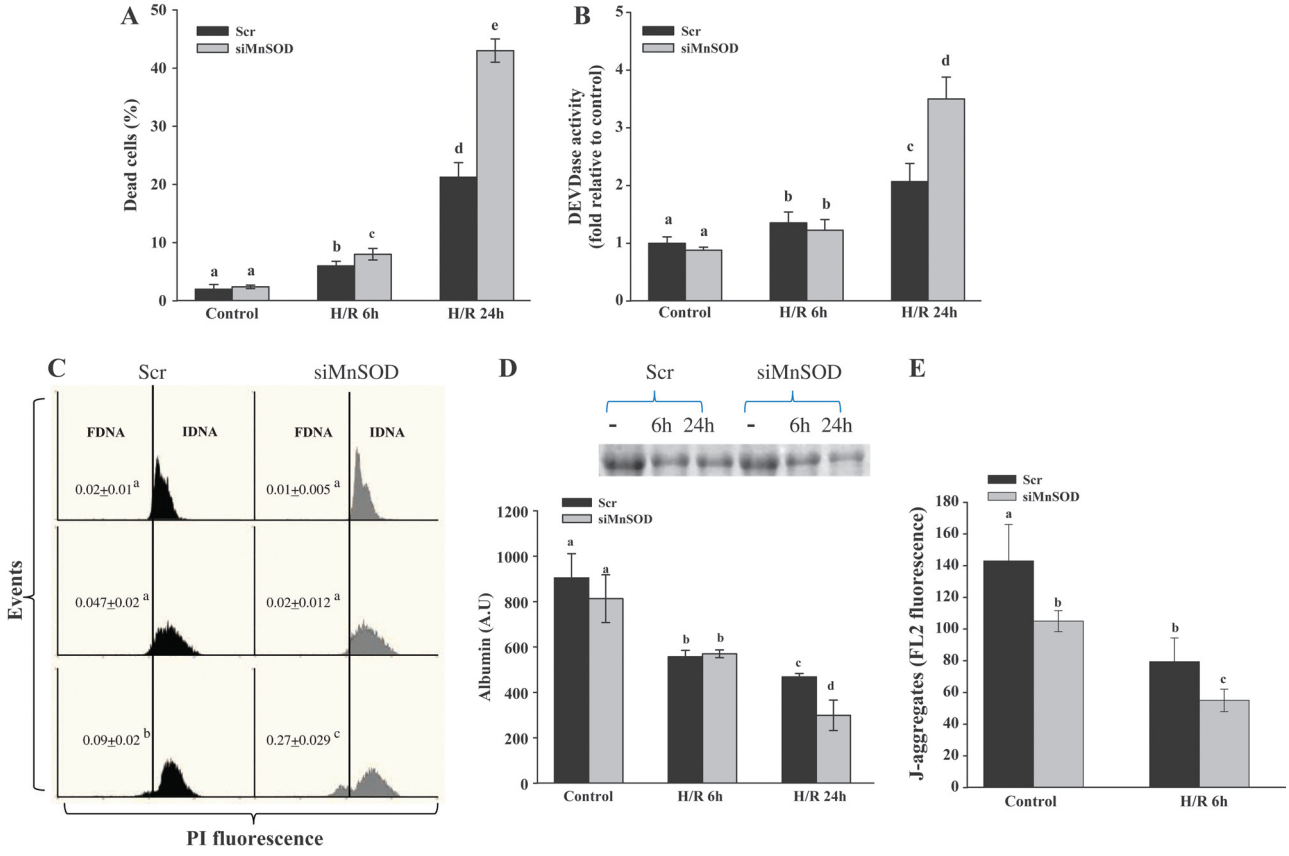

Figure 4. siMnSOD AML-12 hepatocytes are more sensitive to H/R-induced apoptosis. Scr-control and siMnSOD cells were exposed to H/R. (A) Fraction of dead PI-positive cells detected by flow cytometry. (B) DEVDase (caspase) activity measured by fluorogenic specific caspase-3 substrate. (C) DNA integrity was detected by flow cytometry. Numbers represent the ratio between fragmented and intact DNA (FDNA/IDNA). Means with different letters are significantly different at $p < 0.05$, $n = 5$. Histograms are representative of two separate experiments with $n = 5$ in each experiment. (D) SDS-PAGE and coomassie brilliant blue staining: bands of ~70 kDa were excised and subjected to MS for identification, illustrated 85% homology to albumin levels. (E) Cells were tested for loss of mitochondrial membrane potential using JC-1 probe. JC-1–positive aggregates were detected by flow cytometry in Scr-control and siMnSOD cells exposed to H/R for 6 h. Data represent means ± SD; Means with different letters are significantly different at $p < 0.05$. These experiments were performed in triplicate and were repeated twice.

24 h, Figure 4B): enhanced caspase activity (175%) was found in siMnSOD cells after 24 h compared to their Scr-control (Figure 4B). Furthermore, analysis of DNA status indicated a 300% increase in DNA fragmentation in siMnSOD cells compared to Scr-control cells after exposure to 24 h of H/R (Figure 4C). Images of cells taken following H/R confirmed the observed increase in cell death in siMnSOD cells compared to their Scr-controls at 24 h of H/R, demonstrating greater voids between them and an unusual distribution (results not shown) which, again, was not seen in control cells or cells prior to H/R. These results substantiate the physiological role of MnSOD in protecting against H/R injury. Following electrophoresis gel runs, we have noticed the down-regulation of a protein of ~70 kDa. MS analysis identification showed 85% homology to albumin.

Exposing Scr-control and siMnSOD cells to H/R for 6 h reduced albumin levels by 40 and 30%, respectively; however, at 24 h of H/R, there was a significant decrease in the albumin levels of siMnSOD cells: 65% compared to 40% in the Scr-control (Figure 4E). These results support the role for MnSOD in maintaining hepatocyte survival and in regulating vital performance of the hepatocytes, like albumin production during stress. It may be that MnSOD generates its pro-survival signalling effect by releasing ROS from the mitochondria; however, ROS production is very much dependent on $\Delta\psi m$ [19]. Therefore, to further elucidate the role of MnSOD in H/R, $\Delta\psi m$ was measured in siMnSOD cells subjected to H/R. It is interesting to note that, prior to H/R, siMnSOD cells showed considerably lower $\Delta\psi m$ than their Scr-control (Figure 4E). Moreover, following 6 h of H/R, siMnSOD cells demonstrated a stronger reduction in $\Delta\psi m$ (Figure 4E). CCCP, an uncoupler, was used as a control for the measurement, significantly reduced $\Delta\psi m$ in WT-AML-12 cells (results not shown). Therefore, MnSOD role is to maintain $\Delta\psi m$.

Table II. Selected down-regulated genes in siMnSOD cells.

Probe ID	Gene name	Gene symbol	Expression (%)	Raw data Log2 of mean expression	SD
10563597	Serum amyloid A-3 protein precursor, serum amyloid A 3	Saa3	8.8	–3.5	0.11
10514466	Jun oncogene	Jun	18.8	–2.41	0.11
10373358	Interleukin 23, alpha subunit p19	IL23A	20	–2.32	0.27
10523156	Chemokine (c-x-c motif) ligand 2	CXCL2	20	–2.3	0.09
10425283	v-maf musculoaponeurotic fibrosarcoma oncogene family, protein F (avian)	Maff	21	–2.23	0.19
10397346	FBJ osteosarcoma oncogene	Fos	25	–1.96	0.133
10469816	Interleukin receptor antagonist	IL1RN	28	–1.83	0.17
10347888	Chemokine (c-c motif) ligand 20	CCL20	31	–1.68	0.055
10355403	Fibronectin 1	FN1	34	–1.55	0.03
10572897	heme oxygenase (decycling) 1	HO-1	35	–1.5	0.23
10345762	interleukin 1 receptor, type I	Il1r1	35	–1.48	0.3
10441815	Superoxide dismutase, Superoxide dismutase	SOD2	36	–1.47	0.21
10526961	v-maf musculoaponeurotic fibrosarcoma oncogene family, protein K (avian)	Mafk	37	–1.43	0.05
10368144	tumour necrosis factor, alpha-induced protein 3	Tnfaip3	37	–1.4	0.07
10523151	Chemokine (c-x-c motif) ligand 1	Cxcl1	37	–1.4	0.08
10439936	Nuclear factor of kappa light polypeptide gene enhancer in b-cells inhibitor, zeta	NFKBIZ	40	–1.3	0.17
10523595	protein tyrosine phosphatase, non-receptor type 13	Ptpn13	43	–1.2	0.12
10379518	Chemokine (c-c motif) ligand 7	CCL7	43	–1.2	0.015
10391301	Signal transducer and activator of transcription 3	Stat3	45	–1.15	0.07
10379511	Chemokine (c-c motif) ligand 2	CCL2	46	–1.11	0.13
10531420	Chemokine (c-x-c motif) ligand 11	CXCL11	46	–1.1	0.12
0469793	Interleukin 1 family member 6	IL1F6	46	–1.1	0.015
10502299	NF-kappa-B DNA-binding subunit	NFKB1	46	–1.1	0.09
10502299	NF-kappa-B DNA-binding subunit	NFKB1	48	–1.04	0.09
10467921	Chuk conserved helix-loop-helix ubiquitous kinase	Chuk		–0.93	0.08
10460631	v-rel reticuloendotheliosis viral oncogene homolog A (avian)	relA	56	–0.815	0.08
10443463	cyclin-dependent kinase inhibitor 1A (P21)	CDK1a	57	–0.8	0.02

Gene chip data analysis scheme used to identify differentially expressed genes in siMnSOD cells

To characterize MnSOD-mediated protection in H/R of mouse hepatocytes and to obtain a comprehensive understanding of the genome-wide effects in cells silenced for MnSOD, DNA microarray analysis was conducted. Representative data were collected from three independent cell batches and a total of 28 853 probe sets were screened. siMnSOD cells exhibited altered expression compared to their Scr-control that included down-regulation of 470 and up-regulation of 290 genes. An itemized list of the affected genes is presented in Tables II and III, respectively. Results of the microarray experiment shed critical light on the mechanism governing MnSOD-mediated protection. A group of genes down-regulated in siMnSOD cells was related to stress-induced gene expression related to Nrf2, among them HO-1, Fos, MafF, MafK and Jun (Table II), which are involved in Nrf2 signalling. Two other major groups of genes that were down-regulated in siMnSOD cells were related to thenuclear factor-kappa B (NF-kB) signalling pathway, among them NFkB1, Tnfaip3 and Ptpn13 and to the inflammatory response (IL23A, CXCL2, CCL20, Cxcl1, CCL2, CXCL11, FN1 and CCL7, among others) (Table II). Among the genes that were induced in siMnSOD cells were those related to cyclin and cell-cycle regulation (E2F1, CDKn2c, CDK2) (Table III) and those related to lipid metabolic processes (FDFT1, Nsdhl, Idi1, ACAA2, ACLY, TM7SF2, HMGCS1, PMVK) (Table III). To validate the DNA microarray results, the expression of selected siMnSOD-sensitive genes was independently determined using real-time PCR (Figure 5). Using this approach, it was found that the microarray approach under-estimates the magnitude of the change while reliably detecting its direction. Thus, real-time PCR was performed on some of the genes from the group related to oxidative stress via Nrf2. mRNA levels of HO-1 were reduced by more than 70% in siMnSOD cells compared to their Scr-controls (Figure 5A), in agreement with the

Table III. Selected upregulated genes in siMnSOD cells.

Probe ID	Gene name	Gene symbol	Expression (%)	Raw data Log2 of mean expression	SD
10562563	cyclin E1	Ccne1	500	2.32	0.19
10377405	aurora kinase B	Aurkb	482	2.27	0.08
10504470	maternal embryonic leucine zipper kinase	MELK	446	2.16	0.03
10488785	E2F transcription factor 1	E2f1	348	1.8	0.1
10420730	farnesyl diphosphate farnesyl transferase 1	FDFT1	324	1.7	0.05
10600082	NAD(P) dependent steroid dehydroge nase-like	Nsdhl	320	1.68	0.09
10482762	Isopentenyl pyrophosphate isomerase 1	Idi1	303	1.6	0.19
10412466	3-hydroxy-3-methylglutaryl-Coenzyme A synthase 1	HMGCS1	273	1.45	0.11
10515090	cyclin-dependent kinase inhibitor 2C (p18, inhibits CDK4)	Cdkn2c	273	1.45	0.12
10493548	phosphomevalonate kinase	PMVK	263	1.4	0.13
10581479	sphingomyelin phosphodiesterase 3, neutral	SMPD3	246	1.3	0.1
10497831	cyclin A2	Ccna2	246	1.3	0.045
10493548	mevalonate kinase	MVK	246	1.3	0.1
10524266	protein kinase Chk2	Chek2	246	1.3	0.04
10506571	24-dehydrocholesterol reductase	DHCR24	237	1.25	0.05
10376208	GM2 ganglioside activator protein	GM2a	231	1.21	0.15
10466624	aldehyde dehydrogenase family 1, sub-family A7	Aldh1a7	231	1.21	0.01
10401181	Androgen-regulated short-chain dehydrogenase/reductase 1	Rdh11	231	1.21	0.05
10462922	1-phosphatidylinositol-4,5-bisphosphate phosphodiesterase epsilon-1	PLCE1	229	1.2	0.1
10591517	cyclin-dependent kinase inhibitor 2D (p19, inhibits CDK4)	Cdkn2d	229	1.2	0.08
10373530	cyclin-dependent kinase 2	Cdk2	223	1.16	0.05
10373530	cyclin-dependent kinase 2	Cdk2	223	1.16	0.05
10369815	cell division cycle 2 homolog A (S. pombe)	Cdc2a	221	1.15	0.05
10456699	acetyl-Coenzyme A acyltransferase 2 (mitochondrial 3-oxoacyl-Coenzyme A thiolase)	ACAA2	218	1.13	0.05
10587508	Ttk protein kinase	TTK	214	1.1	0.09
10470913	Serine/threonine-protein kinase N3	PKN3	214	1.1	0.23
10478389	Hepatocyte nuclear factor 4 alpha	Hnf4a	214	1.1	0.11
10506714	Low-density lipoprotein receptor-related protein 8	Lrp8	214	1.1	0.01
10391146	ATP citrate lyase	ACLY	200	1.0	0.02

micro-array analysis. GCLC mRNA levels were reduced by 50% compared to their Scr-controls (Figure 5B) and Nrf2 showed a 30% reduction in mRNA levels (Figure 5C).

Signalling through Nrf2 pathway in siMnSOD were evaluated and compared with Scr-control cells. Confocal laser microscopy was used for localization of Nrf2 in the nucleus or the cytosol. Fluorescence intensity was used to evaluate the protein expression level. It is interesting to note that siMnSOD cells showed considerably lower Nrf2 staining compared to Scr-control cells, as indicated by the weak fluorescence intensity (green fluorescence) in siMn-SOD cells (Figure 6A). In addition, the capacity of Nrf2 translocation to the nucleolus is impaired in siMnSOD cells, as treatment with 1 mM H_2O_2 demonstrated little Nrf2 nuclear translocation in siMnSOD cells (Figure 6A). These results suggest that MnSOD act as a signalling mediator for the activation of survival genes following H/R injury in hepatocytes. To further elucidate this point, real time PCR was performed on siMnSOD cells subjected to H/R. siMnSOD cells showed considerably lower Nrf2 and GCLC transcription levels than their Scr-control (Figure 5). Following exposure to 6 h H/ R, siMnSOD cells show no change in Nrf2 (Figure 6B) and GCLC (Figure 6C) mRNA levels, while Scr-control cells subjected to H/R show up-regulation in Nrf2 (Figure 6B) and GCLC (Figure 6C) mRNA levels, thus substantiating the inability of siMnSOD cells to activate Nrf2 signalling. Low Nrf2 expression levels in siMnSOD cells was also confirmed by immunoblotting analysis from total cells protein extraction (nucleus and cytosol) and impaired

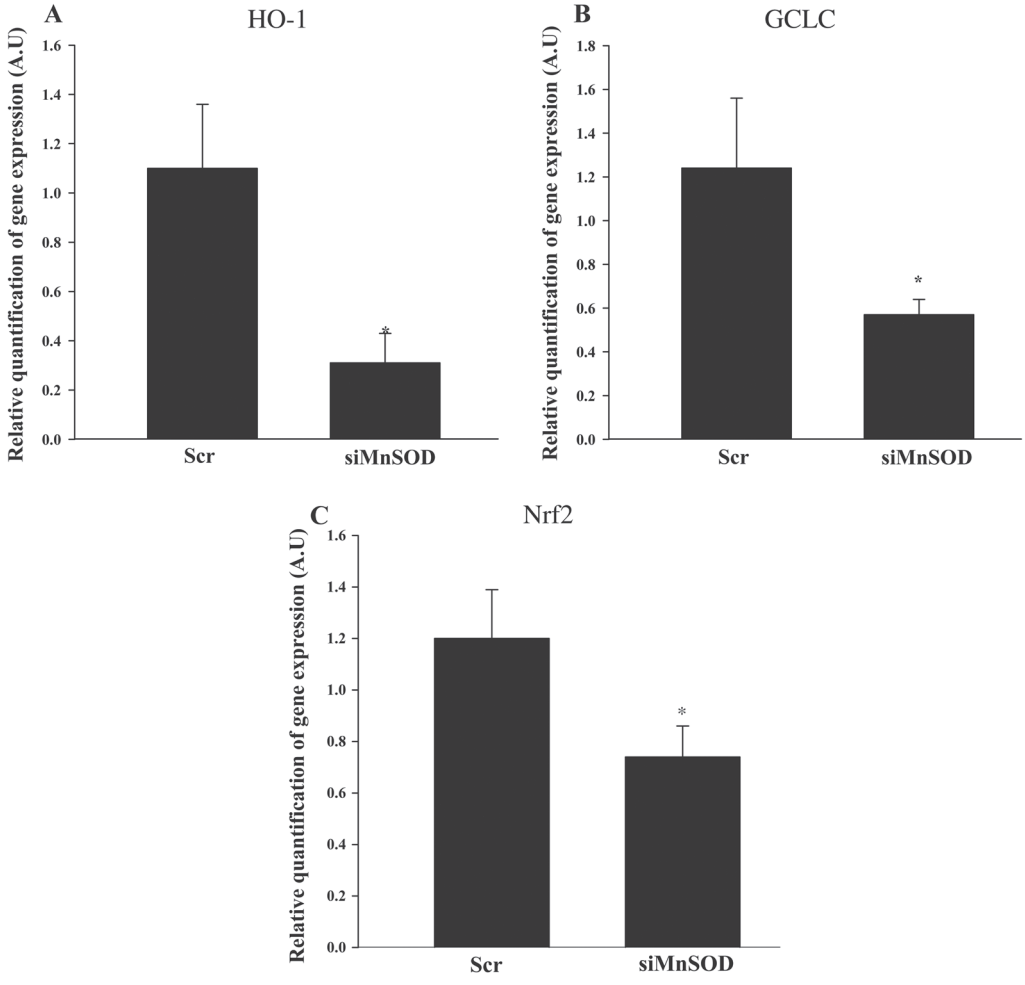

Figure 5. Real-time PCR analysis of selected genes' expression. Quantitative analysis was performed by RTand real-time PCR for mRNA levels of (A) HO-1 gene, (B) GCLC gene and (C) Nrf2 gene. Values are expressed as fold change of gene expression compared to a calibrator (endogenous control, β). Data represent means ± SD; *significantly lower at $p < 0.05$ than controls. These experiments were performed in triplicate and were repeated twice.

localization by cell fractionation (Figure 6D and 6E, respectively). These data indicate that MnSOD supports survival through the activation of transcription factor Nrf2.

Reductions in GSH and lipid peroxidation product levels are observed in siMnSOD cells after H/R

Since GCLC expression levels were down-regulated in siMnSOD cells, intracellular levels of total GSH and GSSG from WT-AML-12 cells were determined by HPLC following H/R. The levels of total GSH decreased from 6 h of H/R to a minimum (45% reduction) at 24 h (Figure 7A). In contrast, GSSG was not detected. Since siMnSOD cells were expected to have an altered redox status, intracellular levels of total GSH were determined in these cells as well. Interestingly, basal levels of GSH (prior to H/R) were different between Scr-control and siMnSOD cells (in accordance with the gene-expression profile): siMnSOD cells had 50% less GSH than their controls (Figure 7A). Moreover, following 24 h of H/ R, GSH levels were greatly diminished in siMnSOD cells compared to their Scr-controls (Figure 7A).

Again, no GSSG was detected in either cell type. The lower GSH content in siMnSOD cells compared to their Scr-control, with no associated increase in GSSG content, suggested that the cells had not been subjected to oxidative stress and that their phenotype of low GSH was largely related to the signalling properties of MnSOD on the glutathione synthesis relevant genes. To further evaluate this possibility, an antibody against 4-HNE-modified proteins was used to determine whether the cells had been subjected to oxidative stress. WT-AML-12 hepatocytes cells labelled with antibody to 4-HNE protein adduct exhibited a higher labelling density in the absence of H/R (~ 2-fold) relative to that after 6 h H/R (Figure 7B). Moreover, a decrease of similar magnitude in 4-HNE levels was also evident after 24 h of H/R (Figure 7B). Interestingly, siMnSOD cells showed a lower basal level of 4-HNE-labelling density (Figure 7C and D) and following 6 and 24 h of H/R, significantly lower levels of 4-HNE were observed (Figure 7C and D, respectively). This indicates

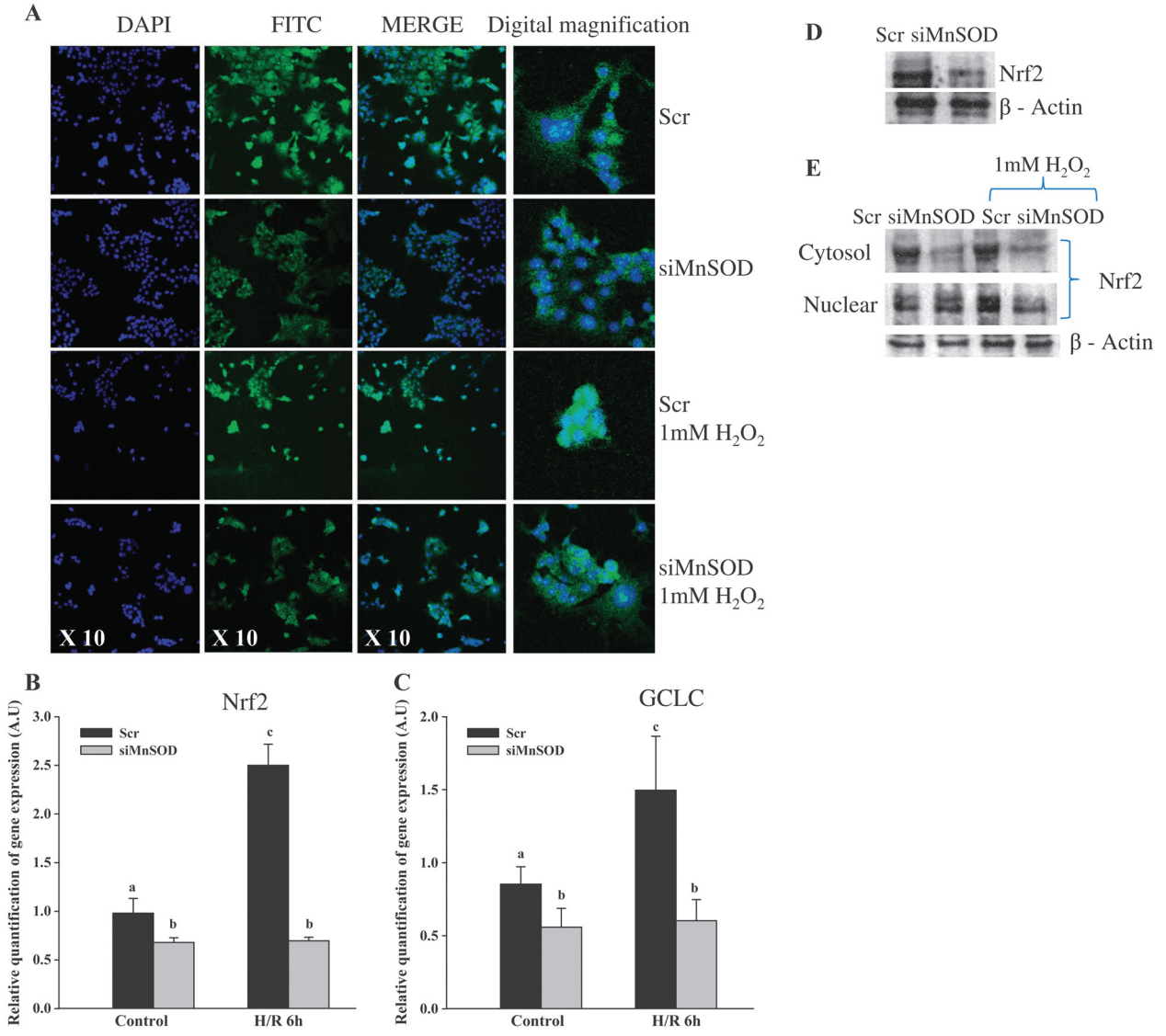

Figure 6. Decreased Nrf2 expression and nuclear translocation are observed in siMnSOD cells. (A) Scr and siMnSOD cells were seeded in eight-well cover-slip chambers and were exposed to 1 mM H2O2 for 2 h. Nrf2 expression and localization is seen as green fluorescence while the nuclei are counterstained with DAPI (in blue). Pictures are representative of two independent experiments. Quantitative analysis was performed by RT and real-time PCR for mRNA levels of (B) Nrf2 gene and (C) GCLC gene. Values are expressed as fold change of gene expression compared to a calibrator (endogenous control, *β*). Data represent means ± SD; Means with different letters are significantly different at $p < 0.05$. Nrf2 expression levels were analysed by immunoblotting with antibodies against Nrf2 and *β* from total cellular extract (D) and fractionation of cytosolic and nuclear extract (E). These experiments were performed in triplicate and were repeated twice.

that siMnSOD cells are more sensitive to H/R conditions; however, they are not under direct oxidative stress according to their lipid peroxidation levels.

Discussion

In this study, the protective mechanism of MnSOD was investigated in H/R injury. H/R is a physiological stress that may activate cell death and damage. This study shows that MnSOD is up-regulated under H/R, this effect is in agreement with our in-vivo finding of increased MnSOD tissue levels following hepatic I/R injury [4]. Inhibition of MnSOD by shRNA confirmed the protein's contribution to increased susceptibility to cell death under H/R. Furthermore, it was observed that MnSOD expression regulates GSH levels probably via the transcription factor Nrf2 and that MnSOD has a role in maintaining hepatocyte cellular function under H/R.

The antioxidative and protective mechanisms triggered by MnSOD over-expression have been previously reported [20,21]. In general, MnSOD is regarded to protect against: cell death [4,22–24], irradiation [25], chromosomal instability [26], diabetes [27], H/R [22,23] or I/R [4], cancers [28] and many other pathological conditions and stress stimuli. The protective effect of MnSOD over-expression against I/R injury was mainly explained via its capacity to

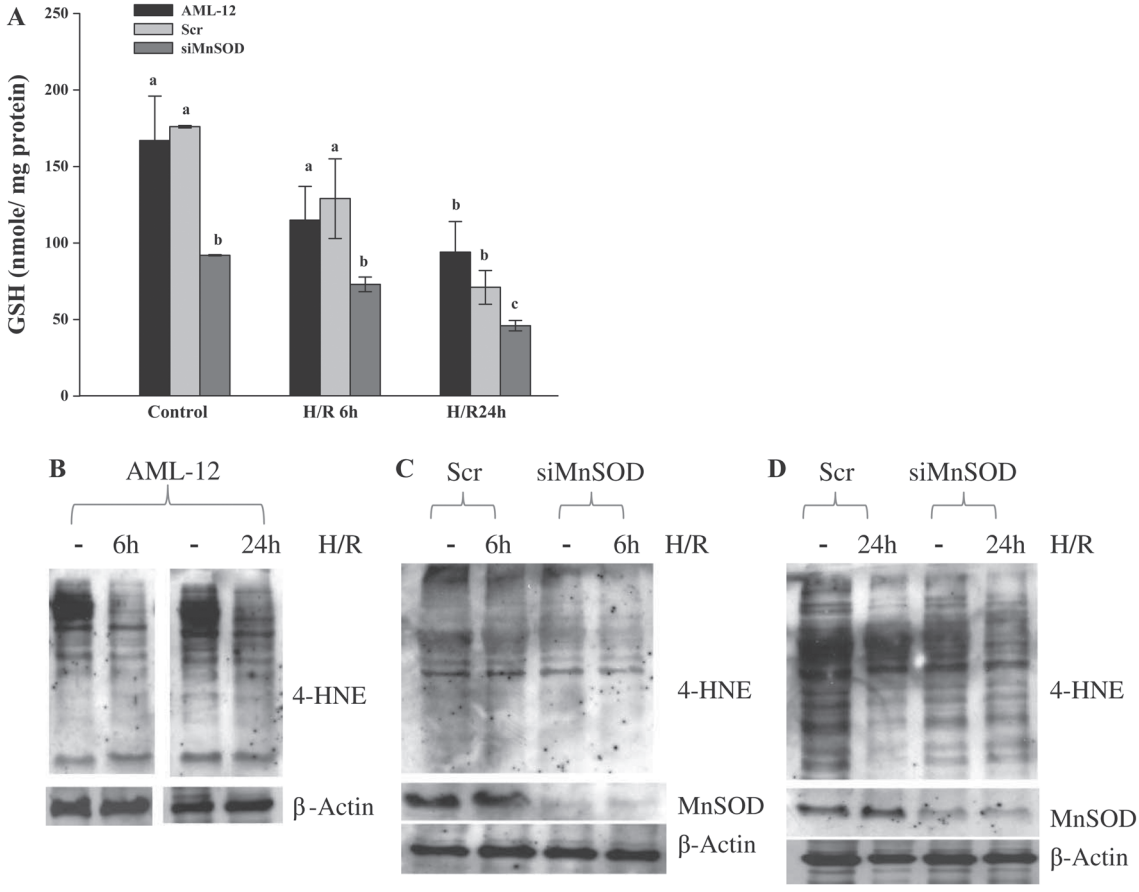

Figure 7. Decreased GSH levels are observed in siMnSOD cells after H/R. Cells were exposed to H/R, GSH content was determined in cell lysates from (A) WT-AML-12 hepatocytes, Scr and siMnSOD cells. Data represent means ± SD from four different experiments; means with different letters are significantly different at $p < 0.05$, $n = 4$. 4–HNE protein adduct levels, a marker of oxidative damage in cells, were determined by immunoblotting with antibodies against 4–HNE and calibrating to β–actin. (B) Analysis of WT-AML-12 cells after 6 and 24 h H/R. Analysis of Scr-control and siMnSOD cells (C) after 6 h of H/R and (D) after 24 h of H/R. Presented lanes represent two different experiments performed in triplicate.

scavenge superoxide radicals from the mitochondria [20,21,23,29]. However, the signalling role of these enzymes and of mitochondrial ROS was not fully addressed. Recently, it has been reported that an increase in the intracellular steady-state production of H_2O_2 by MnSOD can protect against tumour necrosis factor induced apoptosis [30]. This supports our report showing that during activation of FAS receptor (CD95), MnSOD is rapidly degraded as part of the cell death mechanism [17]. During H/ R, a significant portion of the cell-death response is apoptotic. Therefore, a protective effect of MnSOD against H/R could be mediated by a signalling effect on gene expression and adaptation to counteract apoptosis. It is shown here that AML-12 hepatocytes subjected to H/R up-regulate MnSOD; indeed, MnSOD up-regulation during H/R was found to be related to HIF-2alpha activation [31,32].

To shed light on the mechanism by which MnSOD mediates its protection in H/R injury, hepatocytes silenced for MnSOD were subjected to whole-genome microarray analysis. Analysis of the microarray data revealed the altered expression of a group of genes related to Nrf2 signalling, among the most strongly down-regulated being HO-1, Fos, and Jun (Table II). The low expression of these genes in siMnSOD cells suggests a highly-specific and important coordinated response against stress. This response likely involves Nrf2, as this transcription factor has been identified as an activator of these antioxidant genes in different model systems [9,10,13]. Evidence to support this was provided by real-time PCR analysis of Nrf2, GCLC and HO-1 (Figure 5). Expression levels of Nrf2, nuclear translocation capacity and activation of gene expression were found here to be MnSOD dependent (Figure 6). It could be that the flux of H_2O_2 from the mitochondria and cellular redox status which is by part MnSOD dependent regulates transcription of Nrf2 and its activation both under basal conditions and under stress. Recent studies have suggested a link between MnSOD and Nrf2; treatment of human breast epithelial cells with epigalloca-techin-3-gallate induces the expression of GCLC, MnSOD and HO-1, by increasing the transcriptional activity of Nrf2 [33]. An *in-vivo* study using mouse knock-out for the tRNA(Sec) gene (Trsp), in either macrophages

or liver showed elevated H_2O_2 and activated the transcriptional induction of cytoprotective antioxidant genes related to the transcription factor Nrf2 which was related to SOD expression [34]. Another study using microarray following cigarette-smoke-induced oxidative stress in Nrf2(1 /1) mouse lung affirmed an increased number of genes and predicted novel Nrf2 targets, including MnSOD [10], thereby implying a connection between the two proteins. Accumulation of ROS in cells may lead to direct Nrf2 activation and its release to the nucleus [10,12,35]. However, Nrf2 does not attach directly to the promoter of the MnSOD gene but binds to AREs in the promoter region of MnSOD with other transcription factors [12], which would explain MnSOD activation by Nrf2. It is shown here for the first time, by using gene manipulation, that MnSOD expression has a subsequent influence on Nrf2 expression and on the expression of its target genes.

Other possible signalling related to MnSOD-mediated protection was found in a large down-regulated group of genes related to the NF-kB inflammatory response. NF-kB is a transcription factor known to induce both pro-inflammatory and cytoprotective transcripts [36]. It is likely that mitochondria-derived ROS activate NF-kB signalling and, indeed, siMnSOD cells exhibited a lower response to inflammatory stimuli and to the NF-kB pathway, signifying reduced cell survival (Figure 4) after H/R. The presented data suggest that the beneficial effects of MnSOD are due to at least two mechanisms: induction of GCLC and HO-1 via stimulation of Nrf2 and activation of cytoprotective genes by NF-kB activity. These results provide direct proof of the protective signalling potential of MnSOD in H/R and I/R.

GSH is an intracellular peptide with diverse functions that include detoxification, antioxidant defense, maintenance of thiol status and modulation of cell proliferation [37]. H/R attenuates GSH levels in different tissues [38]. siMnSOD cells had low GSH levels and lower GCLC transcription following H/R (Figures 6 and 7), however no increased level of GSSG was detected. Although GSSG may be excluded from the cells into the extracellular medium or get reduced back to GSH, the lack of accumulation of GSSG may also indicate that siMnSOD cells are probably not subjected to increased flux of H_2O_2. GSH is the predominant form in hepatocytes, at concentrations of 5–10 mM in liver cells, while GSSG, which is present at less than 1% the amount of GSH [37]. siMnSOD cells exposed to H/R showed increased sensitivity to the treatment by further decreasing GSH levels (Figure 7). Recently it has been shown that endogenous H_2O_2 generated during muscle differentiation regulates the GSH redox state via activation of the Nrf2 signalling pathway [39]. Hence, MnSOD-derived H_2O_2 in liver cells might represent

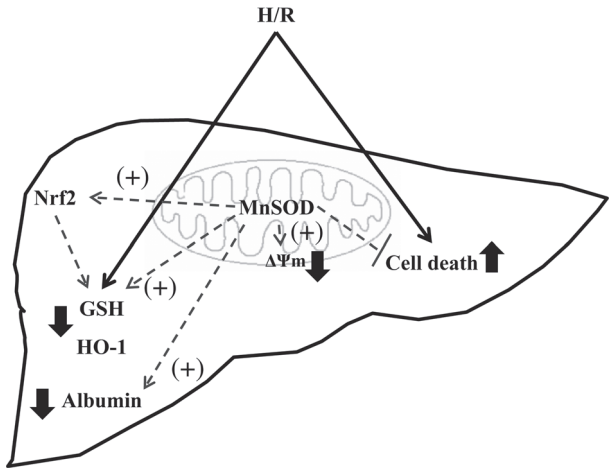

Scheme 1. MnSOD acts as a signalling mediator for survival and functionality. H/R injures cells and mitochondria and as a result, MnSOD is induced. Prolonged elevated MnSOD levels constitute the antioxidant defense in liver hepatocytes and prevent cell death and damage by maintaining $\Delta\psi m$, ROS production and signalling for survival genes. MnSOD up-regulates Nrf2 expression and consequently other antioxidant mediators such as GSH and HO-1. MnSOD also influences liver albumin production, which may preserve liver functionality.

the signalling mediator, acting as a go-between, Nrf2 activation and levels of GSH.

Lipid peroxidation is another practical and effective means of determining oxidative stress and has been found to increase during periods of reoxygenation [40]. Conversely, H/R reduced the levels of 4-HNE in mouse WT-AML-12 hepatocytes. siMnSOD cells had lower lipid peroxidation levels than their Scr-controls, similar to the low levels of lipid peroxidation in cells exposed to H/R. It is likely that reduced production of mitochondrial H_2O_2 subsequent to MnSOD silencing (Figure 3) or to inhibition of respiration due to oxygen deprivation accounts for the low lipid peroxidation levels demonstrated here and in a previous study [41]. These data demonstrate that the protective effect of MnSOD in H/R is more related to its signalling effect on gene expression and adaptation to H/R rather than its direct antioxidant effect. D cm can regulate ROS production [42]. This concept has been demonstrated by the activation of uncoupling protein-2, which moderately stimulates proton leakage across the mitochondrial inner membrane to reduce $\Delta\psi m$ and ROS production [19]. In addition, several papers have reported that overexpression of MnSOD increases D cm [43,44]. Therefore, the connection between low levels of MnSOD and $\Delta\psi m$ was evaluated. Accordingly, siMnSOD cells exhibited a loss of $\Delta\psi m$, which was evident to an even greater extent after H/R (Figure 4E), substantiating MnSOD's role in preserving $\Delta\psi m$. Microarray analysis did not show any alteration in mitochondrial gene expression, indicating a specific effect for MnSOD mitochondrial activity on $\Delta\psi m$

and not on mitochondrial structure. Several mechanisms could account for the effect of MnSOD as a maintainer of hepatocytes D cm: (1) It has been reported that exogenous H_2O_2, the product of MnSOD dismutation, activates the inner membrane space superoxide dismutase-1, delaying loss of transmembrane potential [45]. (2) MnSOD is responsible for the dismutation of superoxide anions with the help of protons, $2H^+ + 2O_2 \rightarrow$ to $H_2O_2+O_2$, and it is therefore possible that by dismutation, MnSOD facilitates the removal of excess protons and thus stabilizes the $\Delta\psi$m.

In summary, the present study elucidates the mechanisms underlying MnSOD protection in H/R injury: H/R damages the cells and MnSOD appears to act as a signalling mediator for survival genes and functionality. Our results suggest that the mechanism of MnSOD upregulation is mediated at least in part by Nrf2 signalling and the regulation of stress response (Scheme 1).

Acknowledgements

This research was supported by a grant from the Dorset Foundation, UK, to O.T.

Declaration of interest: The author reports no conflicts of interest. The author alone is responsible for the content and writing of the paper.

References

[1] Lemasters JJ. The mitochondrial permeability transition and the calcium, oxygen and pH paradoxes: one paradox after another. Cardiovasc Res 1999;44:470–73.

[2] Lemasters JJ, DiGuiseppi J, Nieminen AL, Herman B. Blebbing, free Ca2$^+$ and mitochondrial membrane potential preceding cell death in hepatocytes. Nature 1987;325:78–81.

[3] [3] Fridovich I. Superoxide dismutases: defence against endogenous superoxide radical. Ciba Found Symp 1978;65:77–93.

[4] Pardo M, Budick-Harmelin N, Tirosh B, Tirosh O. Antioxidant defense in hepatic ischemia-reperfusion injury is regulated by damage-associated molecular pattern signal molecules. Free Radic Biol Med 2008;45:1073–1083.

[5] Yang J, Marden JJ, Fan C, Sanlioglu S, Weiss RM, Ritchie TC, Davisson RL, Engelhardt JF Genetic redox preconditioning differentially modulates AP-1 and NF kappa B responses following cardiac ischemia/reperfusion injury and protects against necrosis and apoptosis. Mol Ther 2003; 7:341–353.

[6] Tanaka T, Hakoda S, Takeyama N. Reoxygenation-induced mitochondrial damage is caused by the Ca2$^+$-dependent mitochondrial inner membrane permeability transition. Free Radic Biol Med 1998;25:26–32.

[7] SuYT, Chang HL, Shyue SK, Hsu SL. Emodin induces apoptosis in human lung adenocarcinoma cells through a reactive oxygen species-dependent mitochondrial signaling pathway. Biochem Pharmacol 2005;70:229–241.

[8] Kokoszka JE, Coskun P, Esposito LA, Wallace DC. Increased mitochondrial oxidative stress in the Sod2 (+ / –) mouse results in the age-related decline of mitochondrial function culminating in increased apoptosis. Proc Natl Acad Sci USA 2001;98:2278–2283.

[9] Leonard MO, Kieran NE, Howell K, Burne MJ, Varadarajan R, Dhakshinamoorthy S, Porter AG, O'Farrelly C, Rabb H, Taylor CT Reoxygenation-specific activation of the antioxidant transcription factor Nrf2 mediates cytoprotective gene expression in ischemia-reperfusion injury. Faseb J 2006; 20:2624–2626.

[10] Taylor RC, Acquaah-Mensah G, Singhal M, Malhotra D, Biswal S. Network inference algorithms elucidate Nrf2 regulation of mouse lung oxidative stress. PLoS Comput Biol 2008;4:el000166.

[11] Jaiswal AK. Nrf2 signaling in coordinated activation of antioxidant gene expression. Free Radic Biol Med 2004; 36:1199–1207.

[12] Surh YJ, Kundu JK, Na HK. Nrf2 as a master redox switch in turning on the cellular signaling involved in the induction of cytoprotective genes by some chemopreventive phytochemicals. Planta Med 2008;74:1526–1539.

[13] Kim YJ, Ahn JY, Liang P, Ip C, Zhang Y, Park YM. Human prxl gene is a target of Nrf2 and is up-regulated byhypoxia/reoxygenation: implication to tumor biology. Cancer Res 2007;67:546–554.

[14] Chiu PY, Luk KF, Leung HY, Ng KM, Ko KM. Schisandrin B stereoisomers protect against hypoxia/reoxygenation-induced apoptosis and inhibit associated changes in Ca2$^+$-induced mitochondrial permeability transition and mitochondrial membrane potential in H9c2 cardiomyocytes. Life Sci 2008;82: 1092–1101.

[15] Downey T Analysis of a multifactor microarray study using Partek genomics solution. Methods Enzymol 2006;411: 256–270.

[16] BenjaminiY, Drai D, Elmer G, Kafkafi N, Golani I. Controlling the false discovery rate in behavior genetics research. Behav Brain Res 2001;125:279–284.

[17] Pardo M, Melendez JA, Tirosh O. Manganese superoxide dismutase inactivation during Fas (CD95)-mediated apoptosis in Jurkat T cells. Free Radic Biol Med 2006;41:1795–1806.

[18] Patel V, Chivukula IV, Roy S, Khanna S, He G, Ojha N, Mehrotra A, Dias LM, Hunt TK, Sen CK. Oxygen: from the benefits of inducing VEGF expression to managing the risk of hyperbaric stress. Antioxid Redox Signal 2005;7:1377–1387.

[19] Serviddio G, Bellanti F, Tamborra R, Rollo T, Capitanio N, Romano AD, Sastre J, Vendemiale G, Altomare E. Uncoupling protein-2 (UCP2) induces mitochondrial proton leak and increases susceptibility of non-alcoholic steatohepatitis (NASH) liver to ischaemia-reperfusion injury. Gut 2008; 57:957–965.

[20] DolgachevV, Oberley LW, Huang TT, Kraniak JM, Tainsky MA, Hanada K, Separovic D. A role for manganese superoxide dismutase in apoptosis after photosensitization. Biochem Biophys Res Commun 2005;332:411–17.

[21] Sarsour EH, Agarwal M, Pandita TK, Oberley LW, Goswami PC. Manganese superoxide dismutase protects the prolifera-tive capacity of confluent normal human fibroblasts. J Biol Chem 2005;280:18033–18041.

[22] Haga S, Terui K, Fukai M, Oikawa Y, Irani K, Furukawa H, Todo S, Ozaki M. Preventing hypoxia/reoxygenation damage to hepatocytes by p66(shc) ablation: up-regulation of antioxidant and anti-apoptotic proteins. J Hepatol 2008;48:422–432.

[23] Hirai F, Motoori S, Kakinuma S, Tomita K, Indo HP, Kato H, Yamaguchi T, Yen HC, St Clair DK, Nagano T, Ozawa T, Saisho H, Majima HJ. Mitochondrial signal lacking manganese superoxide dismutase failed to prevent cell death by reoxygenation following hypoxia in a human pancreatic cancer cell line, KP4. Antioxid Redox Signal 2004;6: 523–535.

[24] Xue H, Guo H, LiYC, Hao ZM. Heme oxygenase-1 induction by hemin protects liver cells from ischemia/reperfusion injury in cirrhotic rats. World J Gastroenterol 2007; 13: 5384–5390.

[25] Murley JS, Kataoka Y, Baker KL, Diamond AM, Morgan WF, Grdina DJ. Manganese superoxide dismutase (SOD2)-mediated delayed radioprotection induced by the free thiol form of amifostine and tumor necrosis factor alpha. Radiat Res 2007;167:465–74.

[26] van de Wetering CI, Coleman MC, Spitz DR, Smith BJ, Knudson CM. Manganese superoxide dismutase gene dosage affects chromosomal instability and tumor onset in a mouse model of T cell lymphoma. Free Radic Biol Med 2008; 44:1677–1686.

[27] Kowluru RA, Kowluru V, Xiong Y, Ho YS. Overexpression of mitochondrial superoxide dismutase in mice protects the retina from diabetes-induced oxidative stress. Free Radic Biol Med 2006;41:1191–1196.

[28] Chen CS, Zhao Q, Wang J, Rong JJ, Yuan QS, Guo QL, Wu WT Enhanced anti-tumor effects achieved in a murine tumor model using combination therapy of recombinant human manganese superoxide dismutase and adriamycin. Biochem Biophys Res Commun 2008;370:663–668.

[29] Sarsour EH, Venkataraman S, Kalen AL, Oberley LW, Goswami PC. Manganese superoxide dismutase activity regulates transitions between quiescent and proliferative growth. Aging Cell 2008;7:405–17.

[30] Dasgupta J, Subbaram S, Connor KM, Rodriguez AM, Tirosh O, Beckman JS, Jourd'Heuil D, Melendez JA. Manganese superoxide dismutase protects from TNF-alpha-induced apoptosis by increasing the steady-state production of H_2O_2. Antioxid Redox Signal 2006;8:1295–1305.

[31] [31] Dioum EM, Chen R, Alexander MS, Zhang Q, Hogg RT, Gerard RD, Garcia JA. Regulation of hypoxia-inducible factor 2alpha signaling by the stress-responsive deacetylase sirtuin 1. Science 2009;324:1289–1293.

[32] Scortegagna M, Ding K, Oktay Y, Gaur A, Thurmond F, Yan LJ, Marck BT, Matsumoto AM, Shelton JM, Richardson JA, Bennett MJ, Garcia JA. Multiple organ pathology, metabolic abnormalities and impaired homeostasis of reactive oxygen species in Epasl –/– mice. Nat Genet 2003;35:331–340.

[33] Na HK, Kim EH, Jung JH, Lee HH, Hyun JW, Surh YJ. (–)-Epigallocatechin gallate induces Nrf2-mediated anti-oxidant enzyme expression via activation of PI3K and ERK in human mammary epithelial cells. Arch Biochem Biophys 2008; 476:171–177.

[34] Suzuki T, Kelly VP, Motohashi H, Nakajima O, Takahashi S, Nishimura S, Yamamoto M. Deletion of the selenocysteine tRNA gene in macrophages and liver results in compensatory gene induction of cytoprotective enzymes by Nrf2. J Biol Chem 2008;283:2021–2030.

[35] Seng S, Avraham HK, Birrane G, Jiang S, Li H, Katz G, Bass CE, Zagozdzon R, Avraham S. NRP/B mutations impair Nrf2-dependent NQOl induction in human primary brain tumors. Oncogene 2008;28:378–389.

[36] Partridge J, Carlsen H, Enesa K, Chaudhury H, Zakkar M, Luong L, Kinderlerer A, Johns M, Blomhoff R, Mason JC, Haskard DO, Evans PC. Laminar shear stress acts as a switch to regulate divergent functions of NF-kappaB in endothelial cells. Faseb J 2007;21:3553–3561.

[37] Lu SC. Regulation of glutathione synthesis. Mol Aspects Med 2008;l-2:42–59. [Epub ahead of print].

[38] Fokkelman K, Haase E, Stevens J, Idikio H, Korbutt G, Bigam D, Cheung PY Tissue-specific changes in glutathione content of hypoxic newborn pigs reoxygenated with 21% or 100% oxygen. Eur J Pharmacol 2007;562:132–137.

[39] Ding Y, Choi KJ, Kim JH, Han X, Piao Y, Jeong JH, Choe W, Kang I, Ha J, Forman HJ, Lee J, Yoon KS, Kim SS. Endogenous hydrogen peroxide regulates glutathione redox via nuclear factor erythroid 2-related factor 2 downstream of phosphatidylinositol 3-kinase during muscle differentiation. Am J Pathol 2008;172:1529–1541.

[40] Caraceni P, Rosenblum ER, Van Thiel DH, Borle AB. Reoxygenation injury in isolated rat hepatocytes: relation to oxygen free radicals and lipid peroxidation. Am J Physiol 1994;266:G799–G806.

[41] McDermott BJ, McWilliams S, Smyth K, Kelso EJ, Spiers JP, Zhao Y, Bell D, Mirakhur RK. Protection of cardiomyocyte function by propofol during simulated ischemia is associated with a direct action to reduce pro-oxidant activity. J Mol Cell Cardiol 2007;42:600–608.

[42] Zamzami N, Marchetti P, Castedo M, Decaudin D, Macho A, Hirsch T, Susin SA, Petit PX, Mignotte B, Kroemer G. Sequential reduction of mitochondrial transmembrane potential and generation of reactive oxygen species in early programmed cell death. J Exp Med 1995;182:367–377.

[43] Sutton A, Imbert A, Igoudjil A, Descatoire V, Cazanave S, Pessayre D, Degoul F. The manganese superoxide dismutase Alal6Val dimorphism modulates both mitochondrial import and mRNA stability. Pharmacogenet Genomics 2005; 15:311–319.

[44] Venkataraman S, Jiang X, Weydert C, Zhang Y, Zhang HJ, Goswami PC, Ritchie JM, Oberley LW, Buettner GR. Manganese superoxide dismutase overexpression inhibits the growth of androgen-independent prostate cancer cells. Oncogene 2005;24:77–89.

[45] Inarrea P, Moini H, Han D, Rettori D, Aguilo I, Alava MA, Iturralde M, Cadenas E. Mitochondrial respiratory chain and thioredoxin reductase regulate intermembrane Cu,Zn-superoxide dismutase activity: implications for mitochondrial energy metabolism and apoptosis. Biochem J 2007;405: 173–179.

This paper was first published online on Early Online on 19 October 2009.